Figures and figure supplements

A cell autonomous torsinA requirement for cholinergic neuron survival and motor control

Samuel S Pappas *et al*

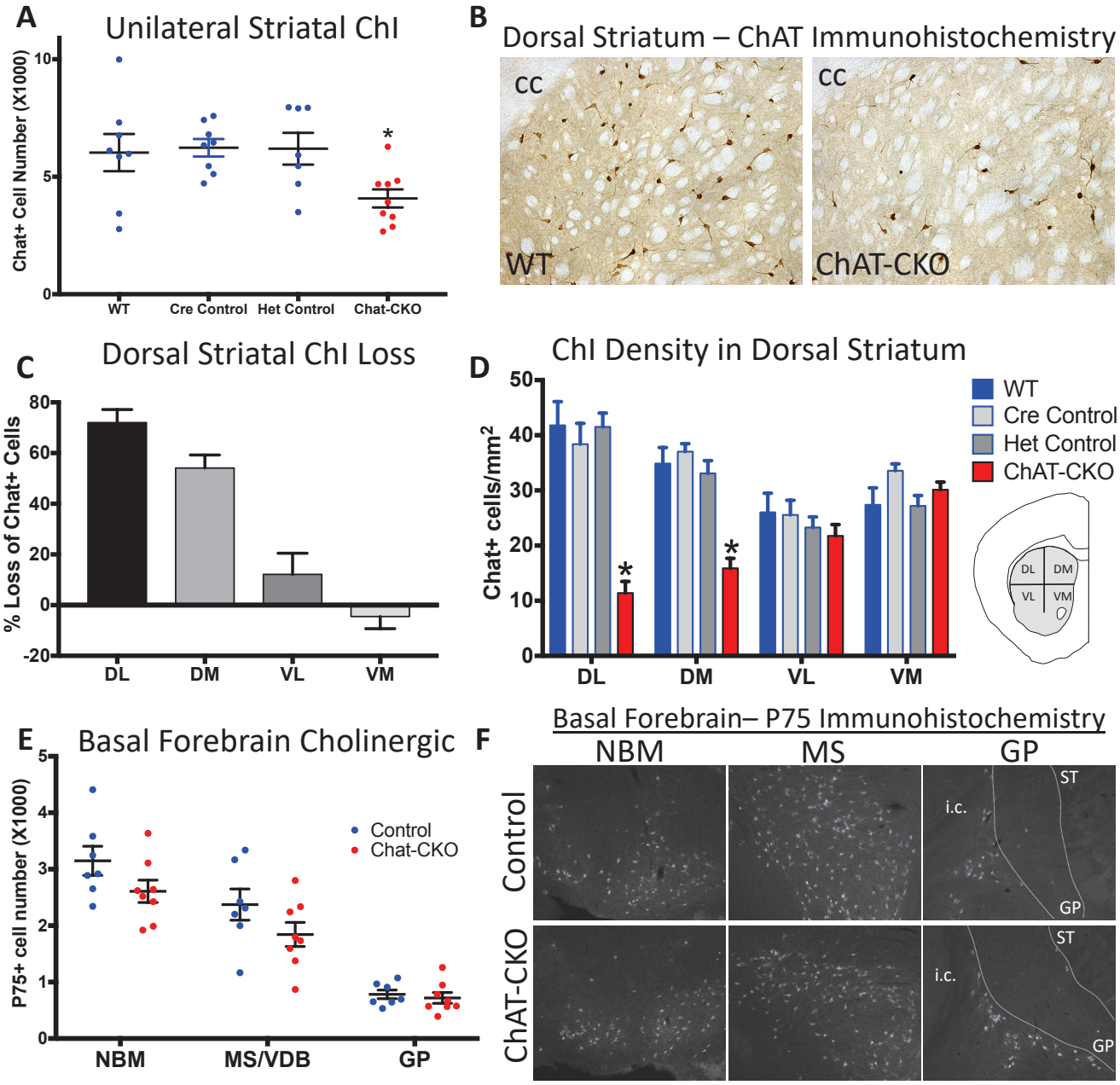

Figure 1. Conditional cholinergic neuron deletion of torsinA causes cell autonomous loss of striatal cholinergic neurons. (**A**) Unilateral stereological quantification of the number of ChAT-positive neurons in the striatum of ChAT-CKO and control mice (One-way ANOVA $F_{(3,28)}$ = 3.589, p=0.02, Dunnett's multiple comparisons test: adjusted p value = 0.049; 'WT'=*Tor1a*$^{Flx/+}$; 'Cre Control'=ChAT-Cre+, *Tor1a* $^{Flx/+}$; 'Het Control'=*Tor1 a*$^{Flx/-}$; 'ChAT-CKO'=ChAT-Cre+, *Tor1a*$^{Flx/-}$). (**B**) ChAT immunohistochemistry of coronal sections containing dorsal striatum from WT and ChAT-CKO mice (cc = corpus callosum). (**C**) Percent reduction in cell density by striatal quadrant (DL = dorsolateral; DM = dorsomedial, VL = ventrolateral, VM = ventromedial). (**D**) Significant ChI loss is selective for dorsal striatal quadrants. Cell density quantification in control and ChAT-CKO striatal quadrants (Two-way ANOVA main effect of genotype $F_{(3,112)}$ = 24.02, p<0.0001; main effect of quadrant $F_{(3,112)}$=8.398, p<0.0001; interaction $F_{(9,112)}$=8.11, p<0.0001. Post-hoc Tukey's multiple comparisons test). (**E**) Basal forebrain neurons are spared in ChAT-CKO mice. Stereological quantification of P75-immunoreactive basal forebrain cholinergic neurons in the nucleus basalis of meynert (NBM), medial septum/nucleus of the vertical limb of the diagonal band (MS/VDB), and globus pallidus (GP). No differences in the number of cholinergic neurons was observed (NBM,

Figure 1 continued on next page

Figure 1 continued

$t_{(13)}$=1.684, p=0.11; MS/VDB, $t_{(13)}$=1.537, p=0.148; GP, $t_{(13)}$=0.5, p=0.625). (**F**) P75 immunohistochemistry of sagittal sections containing basal forebrain cholinergic neuron populations. i.c. = internal capsule, ST = striatum.

DOI: https://doi.org/10.7554/eLife.36691.002

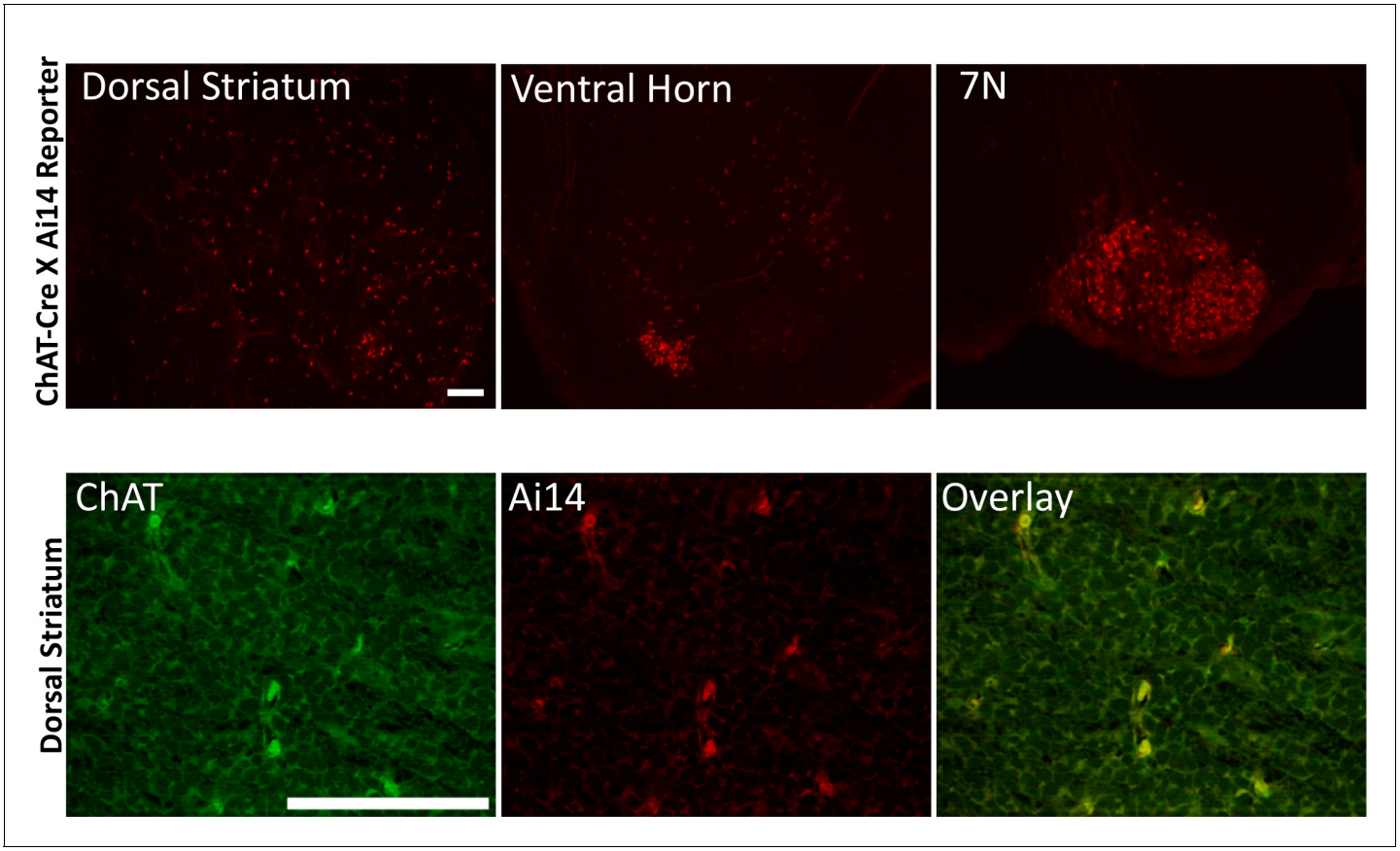

Figure 1—figure supplement 1. ChAT-Cre is expressed prenatally. (Upper panels) ChAT-Cre mice were crossed with Ai14 Cre reporter mice. Offspring were collected immediately after birth, brain sections were generated and observed under epifluorescence microscopy. (Lower panels) adjacent sections costained for torsinA. Scale bar = 50 μm.

DOI: https://doi.org/10.7554/eLife.36691.003

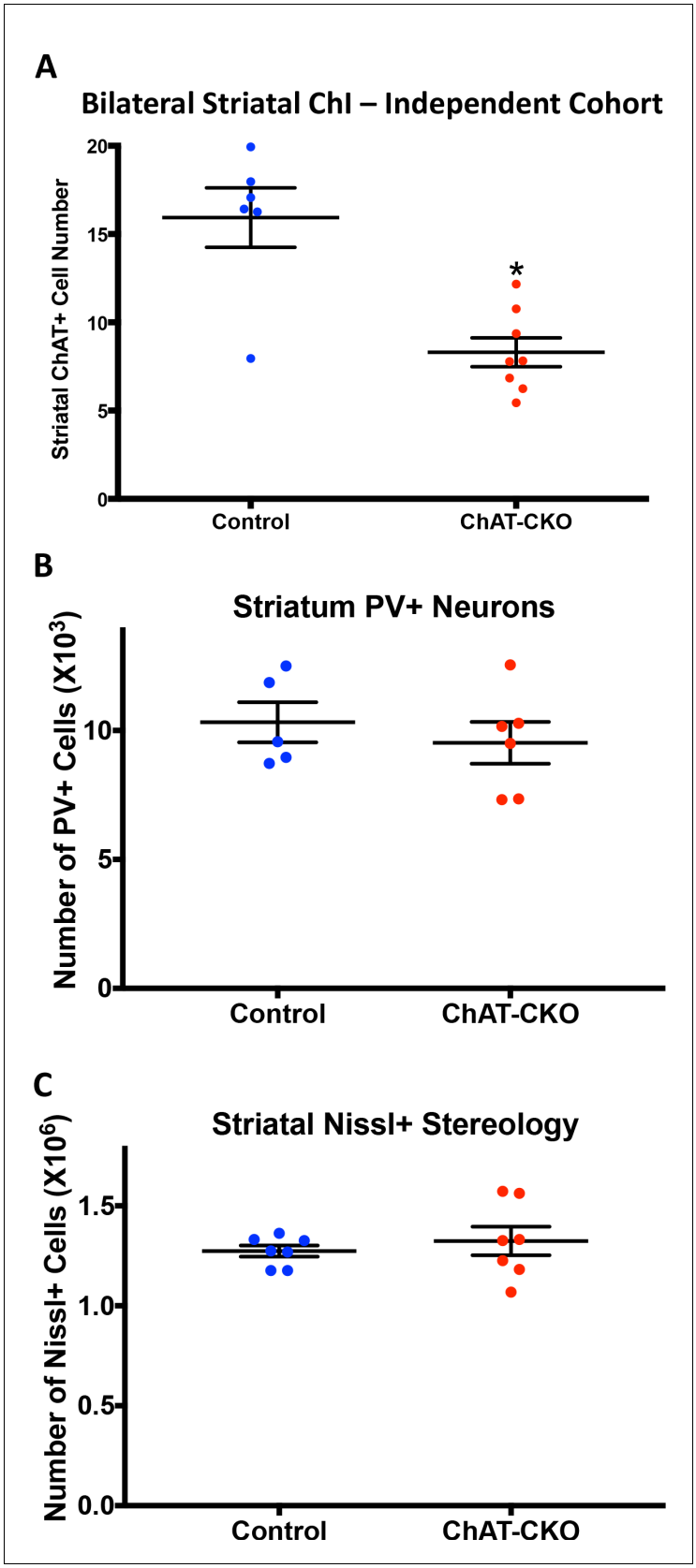

Figure 1—figure supplement 2. Independent cohort confirmation of selective striatal cholinergic neuron loss in ChAT-CKO mice. (**A**) Bilateral unbiased stereology of ChAT-immunoreactive neurons in the dorsal striatum

Figure 1—figure supplement 2 continued on next page

Figure 1—figure supplement 2 continued

($t_{(12)}$=4.42, p=0.0008). (**B**) Unbiased stereology of parvalbumin (PV) immunoreactive neurons in the dorsal striatum (t_9 = 0.699, p=0.50). (**C**) Unbiased stereology of Nissl positive cells in the dorsal striatum (Welch's t-test; $t_{7.803}$=0.655, p=0.53).

DOI: https://doi.org/10.7554/eLife.36691.004

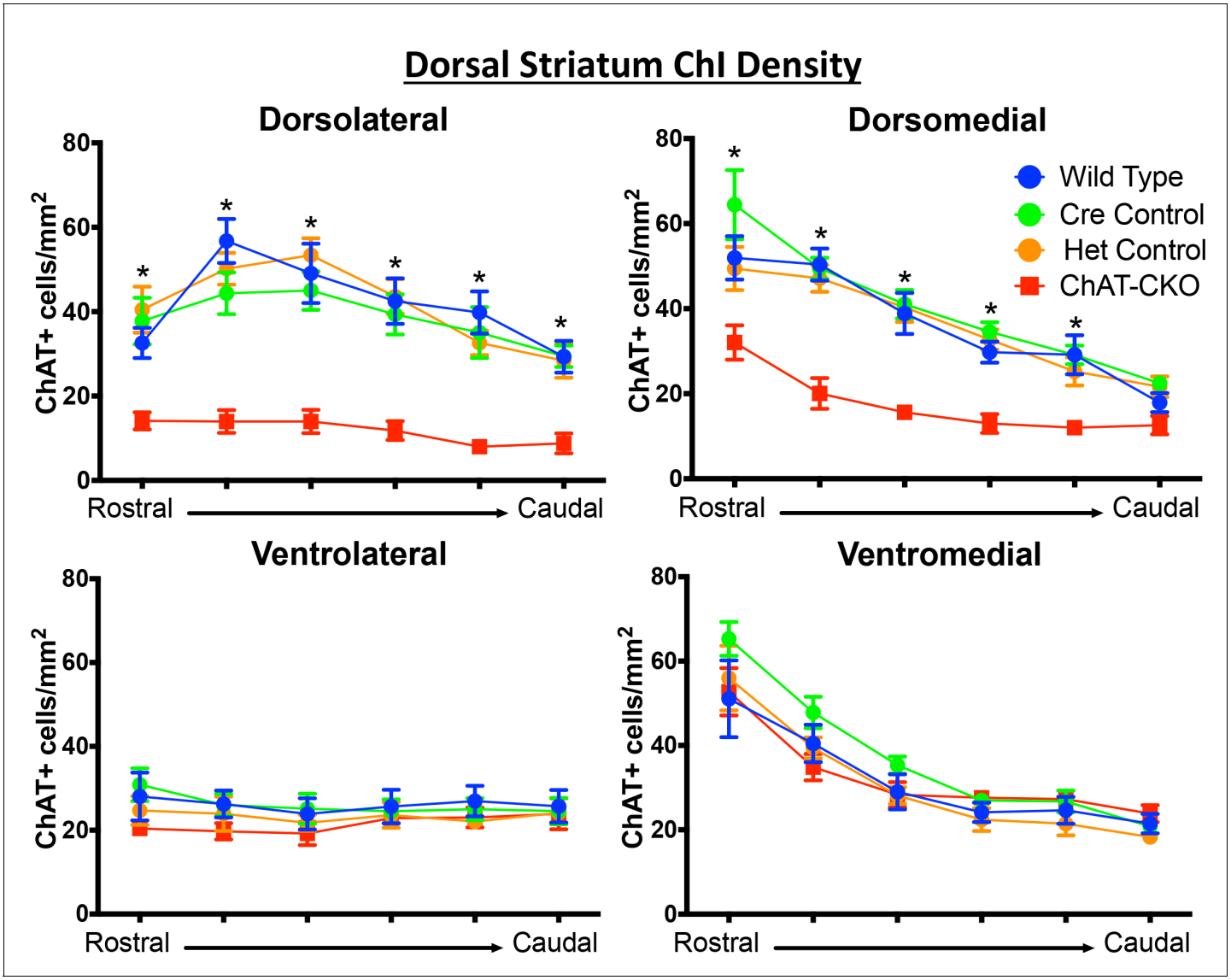

Figure 1—figure supplement 3. ChAT-positive neurons are reduced in a topographic pattern throughout the rostrocaudal extent of the dorsal striatum. Significant decreases in ChAT-positive cells were observed in the dorsolateral and dorsomedial segments of the dorsal striatum (dorsolateral striatum, two-way ANOVA main effect of genotype $F_{(3,156)}$=74.77, p<0.0001, main effect of rostrocaudal section, $F_{(5,156)}$=10.07, p<0.0001, no interaction $F_{(15,156)}$=1.204, p=0.273; Dorsomedial striatum main effect of genotype $F_{(3,156)}$=50.01, p<0.0001, main effect of rostrocaudal section, $F_{(5,156)}$=41.81, p<0.0001, no interaction $F_{(15,156)}$=1.646, p=0.067. Post-hoc Tukey's test was performed for all significant main effects. * represents significant difference between ChAT-CKO mice and all control groups). No significant reductions were observed in the ventral segments of the dorsal striatum (ventrolateral; genotype $F_{(3,156)}$=2.84, p=0.039 [post-hoc Tukey's test adjusted p=0.129 or higher for all comparisons], rostrocaudal section $F_{(5,156)}$=0.479, p=0.79, interaction $F_{(15,156)}$=0.249, p=0.99. ventromedial; genotype $F_{(3,156)}$= 2.706, p=0.047 [post-hoc Tukey's test adjusted p=0.107 or higher for all comparisons], rostrocaudal section $F_{(5,156)}$=46.28 p<0.0001, interaction $F_{(15,156)}$=0.672, p=0.80).

DOI: https://doi.org/10.7554/eLife.36691.005

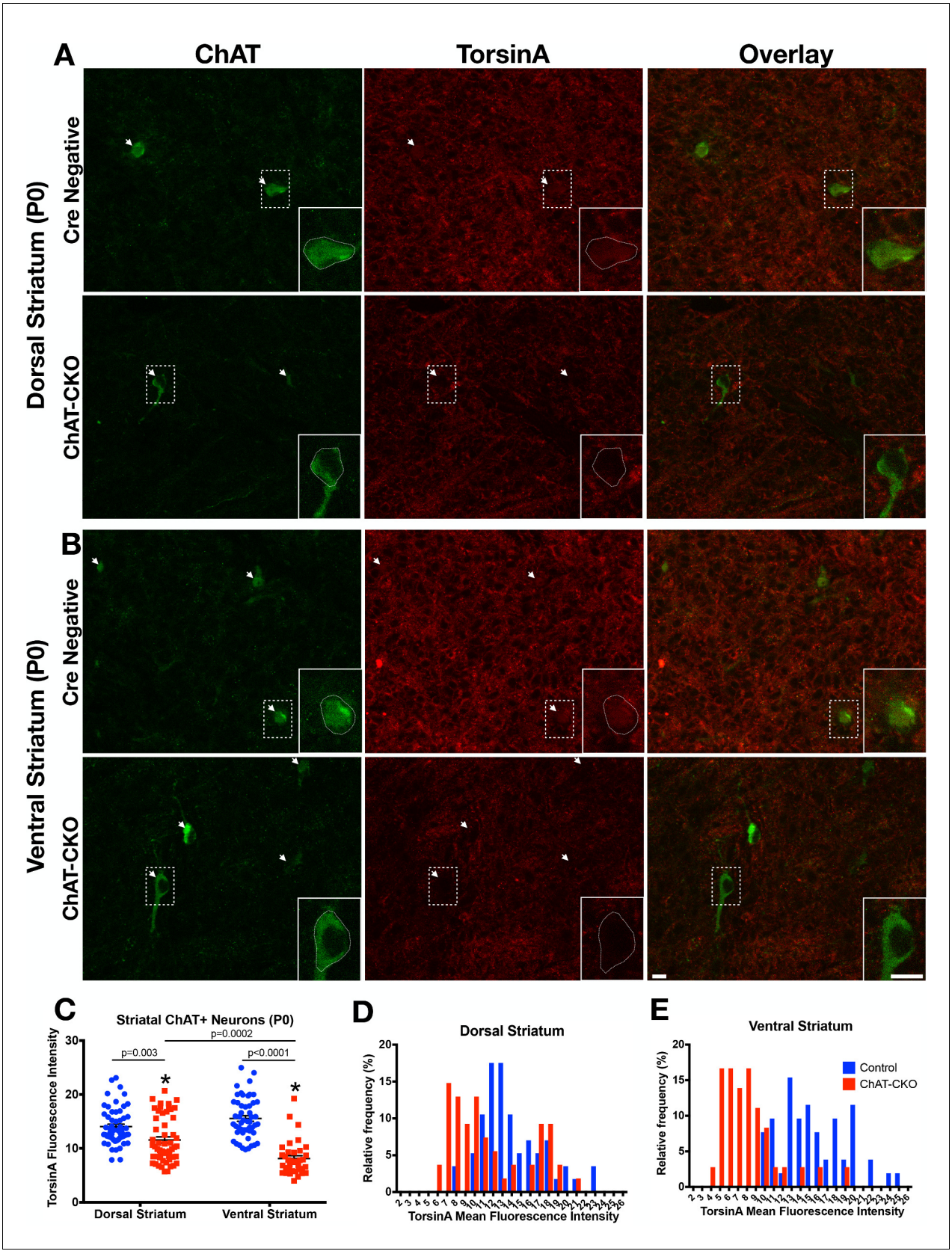

Figure 1—figure supplement 4. Time course of torsinA protein loss in dorsal and ventral striatum. (**A,B**) TorsinA and ChAT staining in dorsal and ventral striatum brain sections from P0 ChAT-CKO and control mice. (**C**) TorsinA mean fluorescence intensity analysis in dorsal or ventral striatal ChI

Figure 1—figure supplement 4 continued on next page

Figure 1—figure supplement 4 continued

(Two-way ANOVA main effect of genotype $F_{1,195}$= 85.67, p<0.0001; Region, n.s., $F_{1,195}$=3.301, p=0.07; interaction $F_{1,195}$=21.34, p<0.0001. Sidak's multiple comparisons test, Dorsal striatum control vs ChAT-CKO, p=0.003, Ventral striatum control vs ChAT-CKO, p<0.0001, ChAT-CKO dorsal striatum vs ventral striatum, p=0.0002; Control dorsal striatum vs ventral striatum, n.s., p=0.199). (**D,E**) Frequency histograms of torsinA mean fluorescence intensity in dorsal (n = 57 control, n = 54 ChAT-CKO neurons) and ventral striatal ChI (n = 52 control, n = 36 ChAT-CKO neurons). Scale bar = 10 μm.
DOI: https://doi.org/10.7554/eLife.36691.006

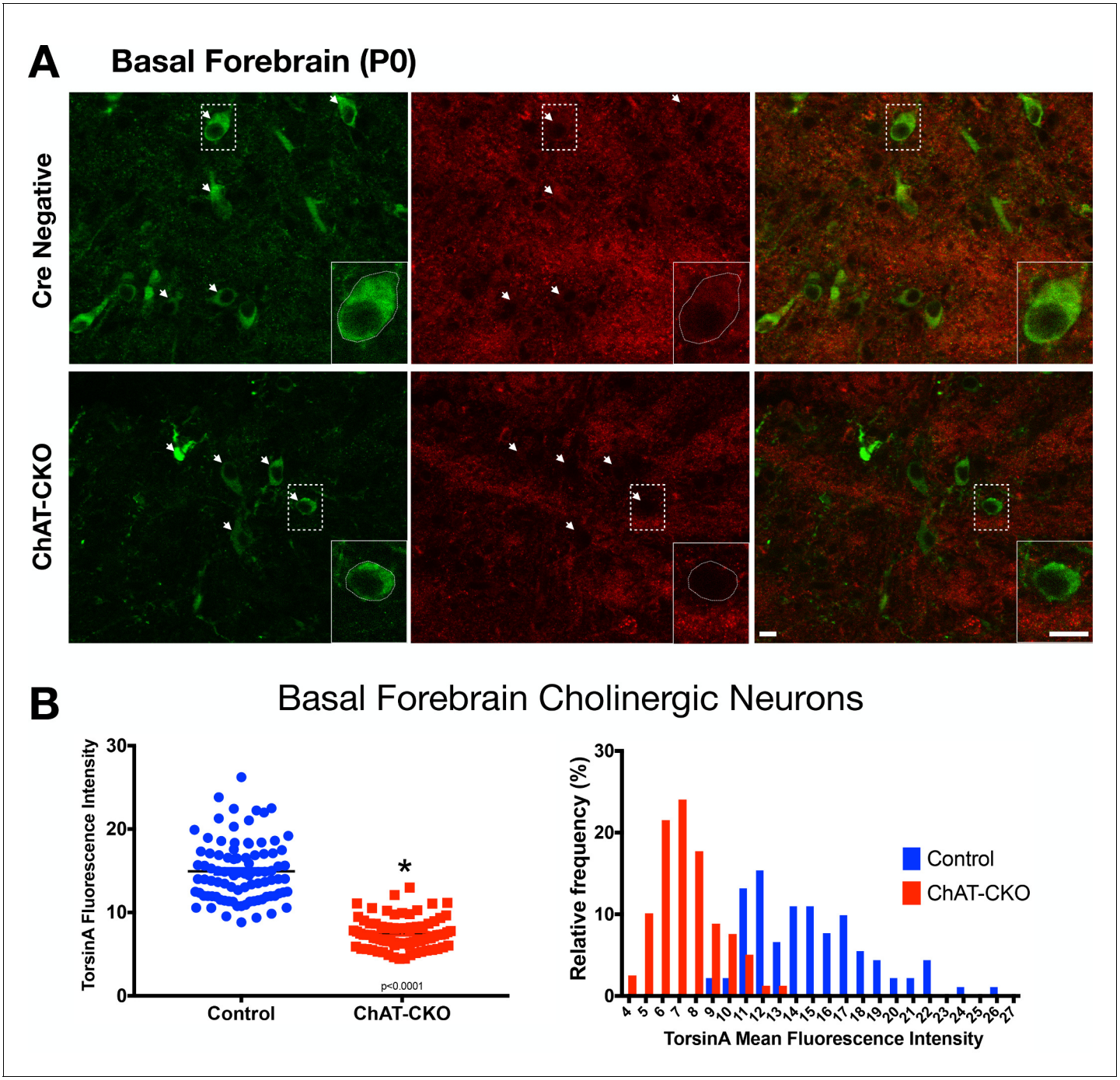

Figure 1—figure supplement 5. Time course of torsinA protein loss in basal forebrain. (**A**) TorsinA and ChAT staining in basal forebrain brain sections from P0 ChAT-CKO and control mice. (**B**) TorsinA mean fluorescence intensity analysis of control and ChAT-CKO (Welch's t-test $t_{138.2}$=17.35, p<0.0001) and frequency histograms of torsinA mean fluorescence intensity in basal forebrain cholinergic neurons ChI (n = 91 control, n = 79 ChAT-CKO neurons). Scale bar = 10 μm.

DOI: https://doi.org/10.7554/eLife.36691.007

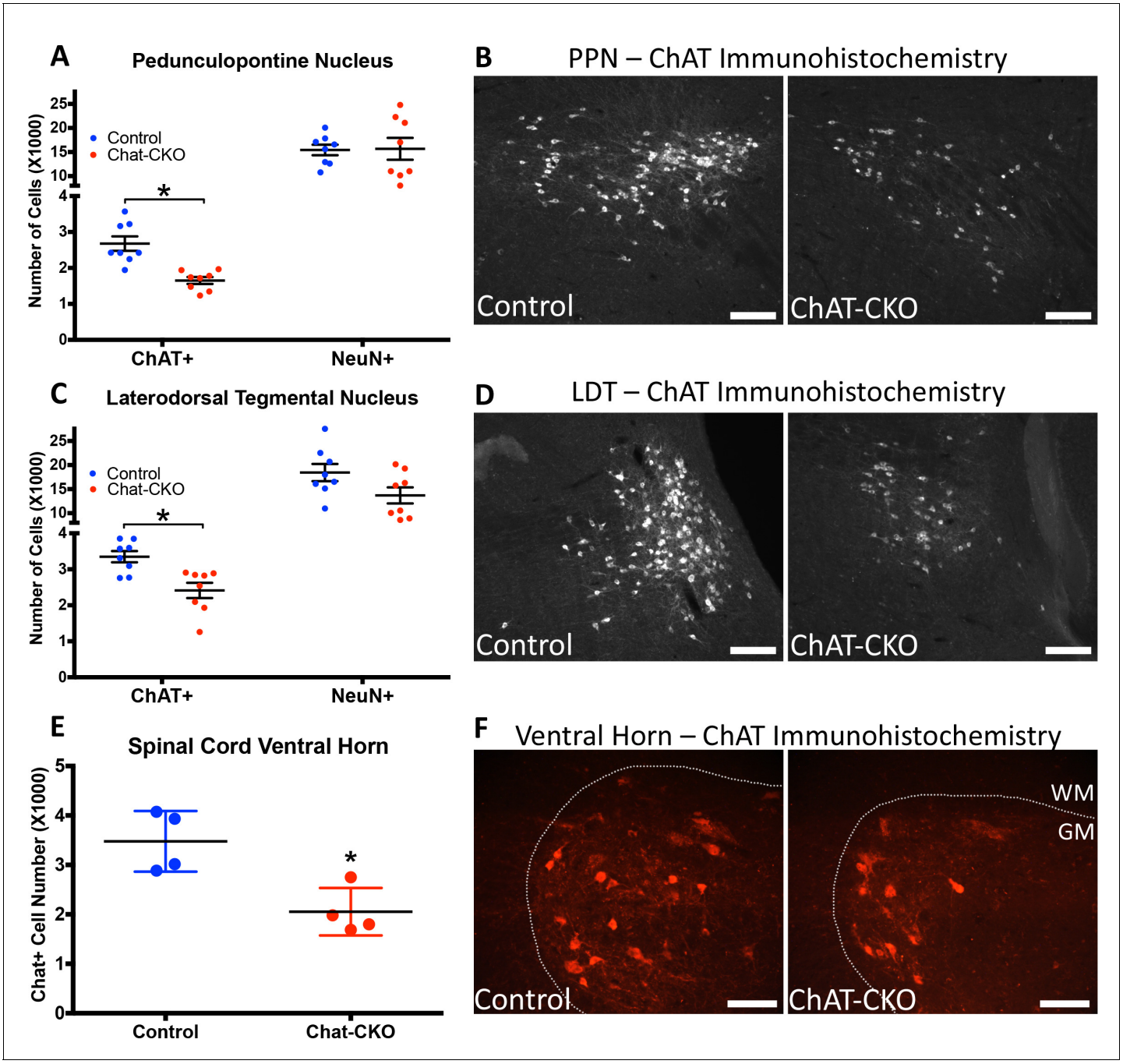

Figure 2. ChAT-CKO mice have significantly fewer brainstem and spinal cord cholinergic neurons. (**A,B**) Stereological quantification of ChAT-positive or NeuN-positive neurons in the pedunculopontine nucleus (PPN) of control and ChAT-CKO mice (ChAT; $t_{(14)}$=4.531, p=0.0005. NeuN; $t_{(14)}$=0.095, p=0.92). (**C,D**) Stereological quantification of ChAT-positive or NeuN-positive neurons in the laterdorsal tegmental nucleus (LDT) of control and ChAT-CKO mice (ChAT; $t_{(14)}$=3.571, p=0.003. NeuN; $t_{(14)}$=1.934, p=0.073). (**E,F**) Quantification of the number of ChAT-positive neurons in the cervical spinal cord of control and ChAT-CKO mice ($t_{(6)}$=3.654, p=0.0107). Scale bars = 100 μm.

DOI: https://doi.org/10.7554/eLife.36691.008

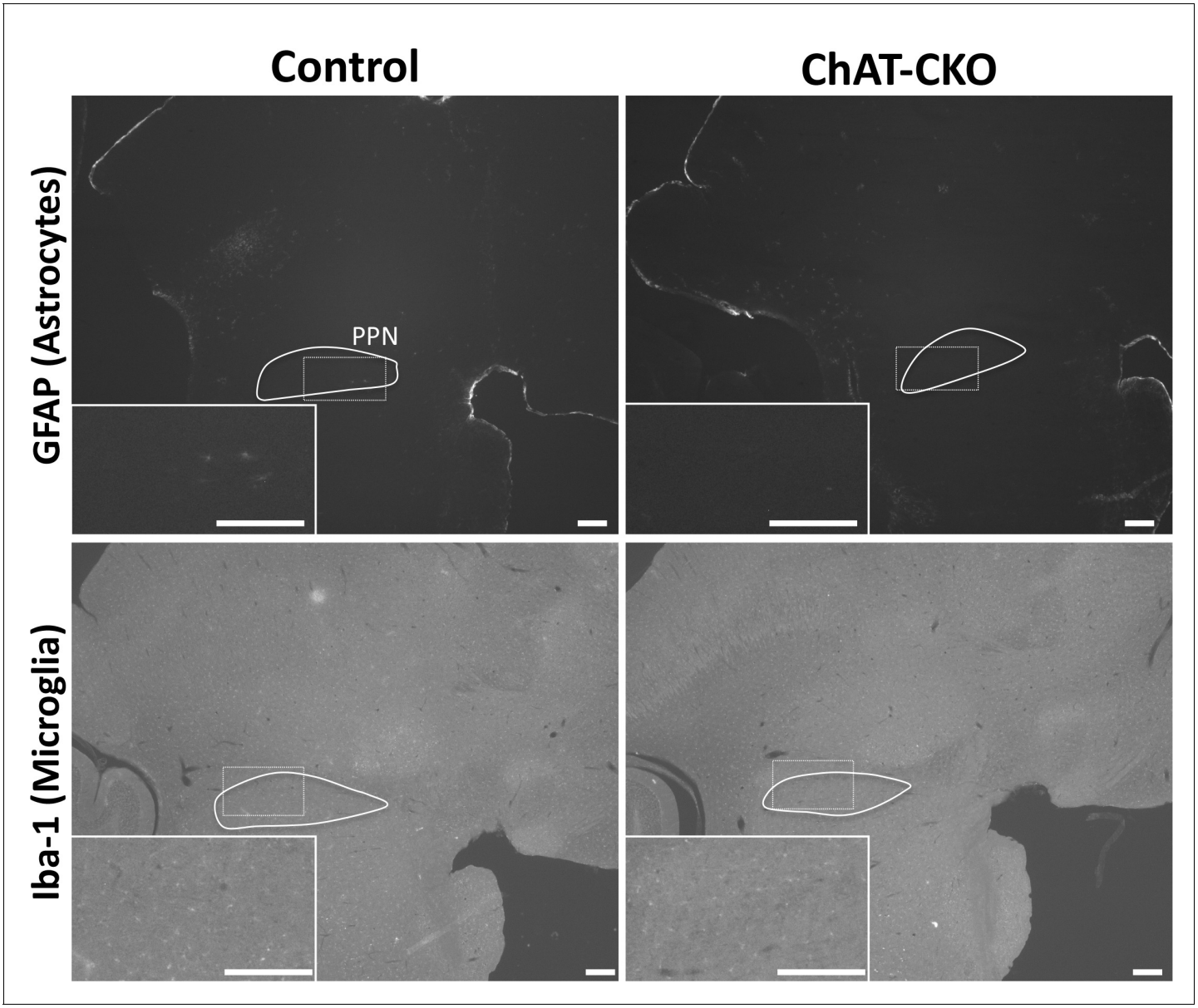

Figure 2—figure supplement 1. Absence of gliosis in the brainstem of ChAT-CKO mice. Immunohistochemistry of GFAP (glial fibrillary acidic protein; specific to astrocytes) and Iba-1 (ionized calcium-binding adapter molecule 1; specific to microglia) in sagittal sections of control and ChAT-CKO hindbrain demonstrate normal distribution of glia.

DOI: https://doi.org/10.7554/eLife.36691.009

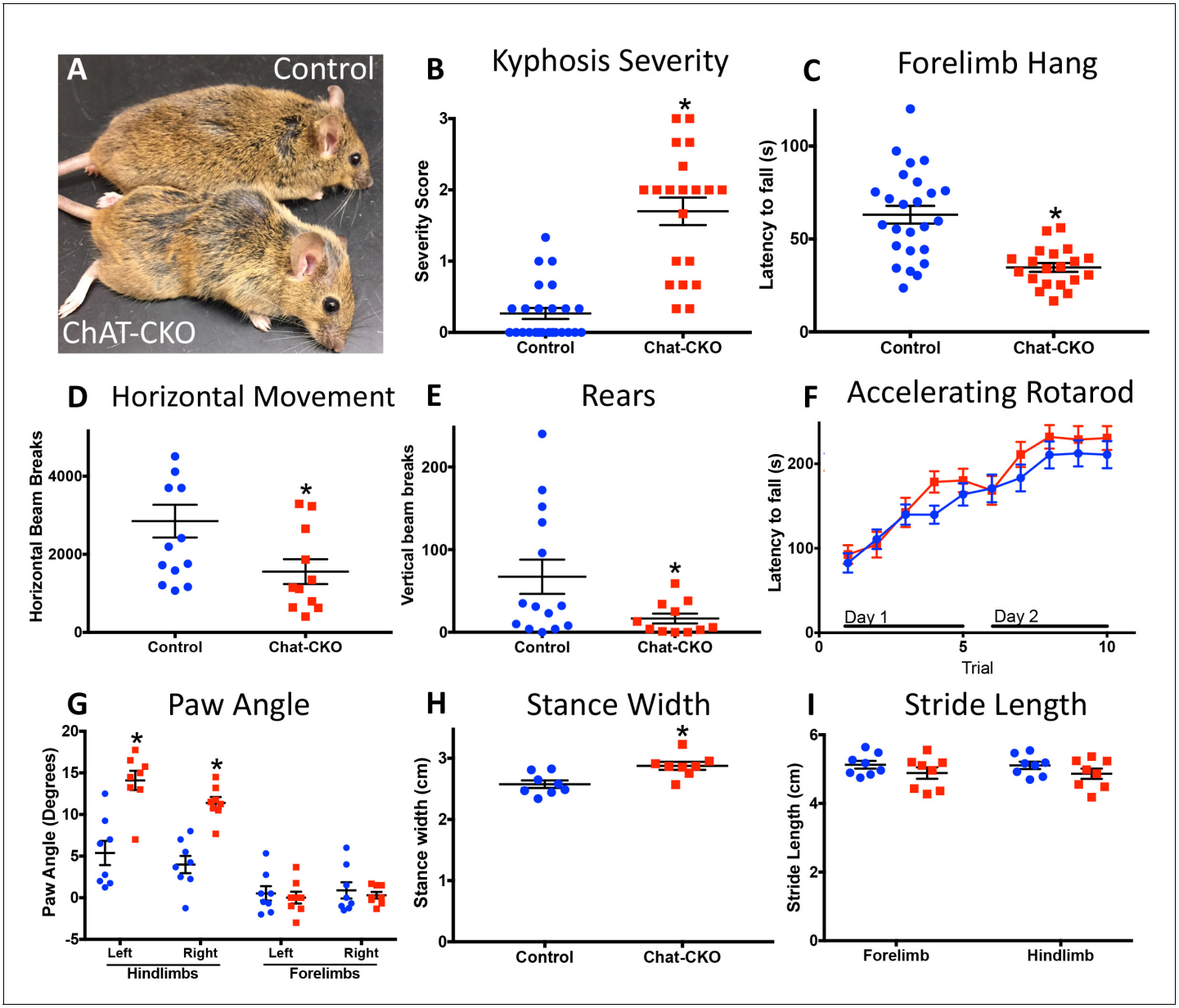

Figure 3. Motor behavior is severely disrupted in ChAT-CKO mice. (**A**) Representative image of a control and ChAT-CKO mouse demonstrates severe kyphosis and unkempt coat. (**B**) ChAT-CKO mice exhibit significantly increased kyphotic curvature during locomotion (Mann-Whitney U = 35, p<0.0001). (**C**) ChAT-CKO mice exhibit a significantly reduced latency to fall during forelimb suspension (Mann-Whitney U = 71.5, p<0.0001). (**D, E**) ChAT-CKO mice are hypoactive in the open field (horizontal movement, $t_{(23)}$=2.345, p=0.028; vertical rears, welch-corrected $t_{(15.1)}$ = 2.345, p=0.033). (**F**) Performance on the accelerated rotarod does not significantly differ from controls (two-way repeated measures ANOVA, genotype, $F_{(1,43)}$=0.75, p=0.389; trial, $F_{(9,387)}$=55.63, p<0.0001; interaction, $F_{(9,387)}$=1.194, p=0.297). (G - I) ChAT-CKO mouse gait is abnormal during locomotion (*paw angle*, two-way ANOVA main effect of genotype, $F_{(1,56)}$=30.54, p<0.0001, main effect of limb $F_{(3,56)}$=51.02, p<0.0001, interaction $F_{(3,56)}$=13.51, p<0.0001, post-hoc Sidak's multiple comparisons test. *Stance width*, $t_{(14)}$=3.329, p=0.005. *Stride length*, two-way ANOVA genotype $F_{(1,28)}$=3.164, p=0.086, limb $F_{(1,28)}$=0.02, p=0.887, interaction $F_{(1,28)}$=0.0001, p=0.989).

DOI: https://doi.org/10.7554/eLife.36691.010

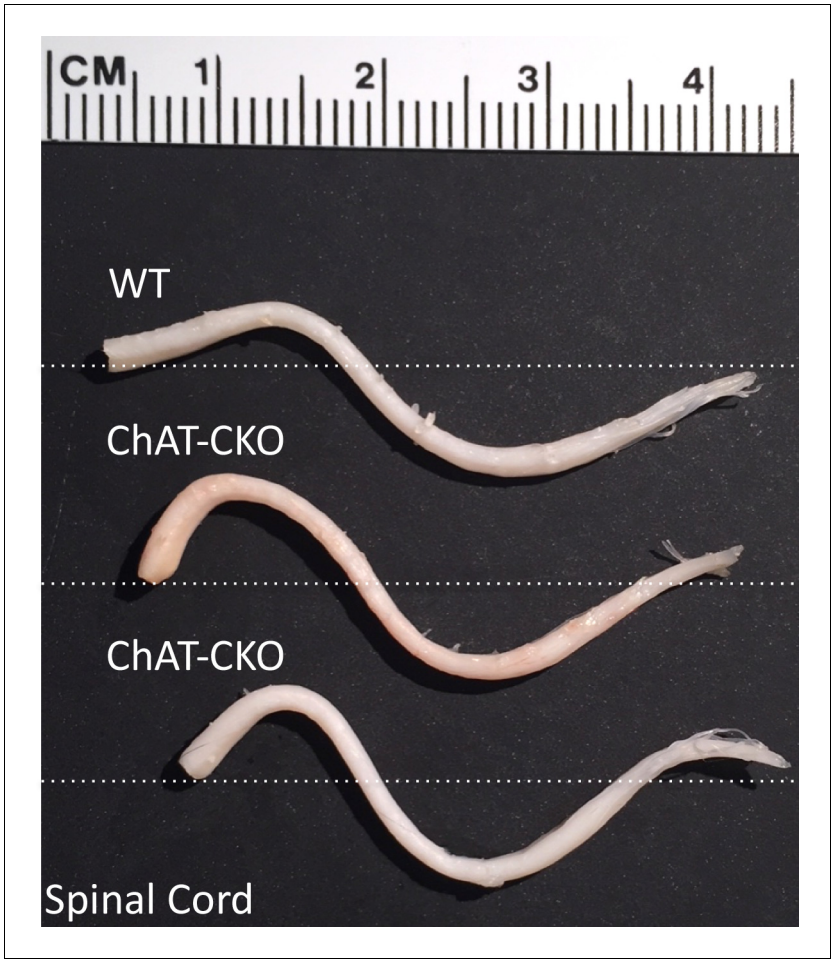

Figure 3—figure supplement 1. Representative examples of control and ChAT-CKO spinal cords demonstrate significant kyphotic curvature.

DOI: https://doi.org/10.7554/eLife.36691.011

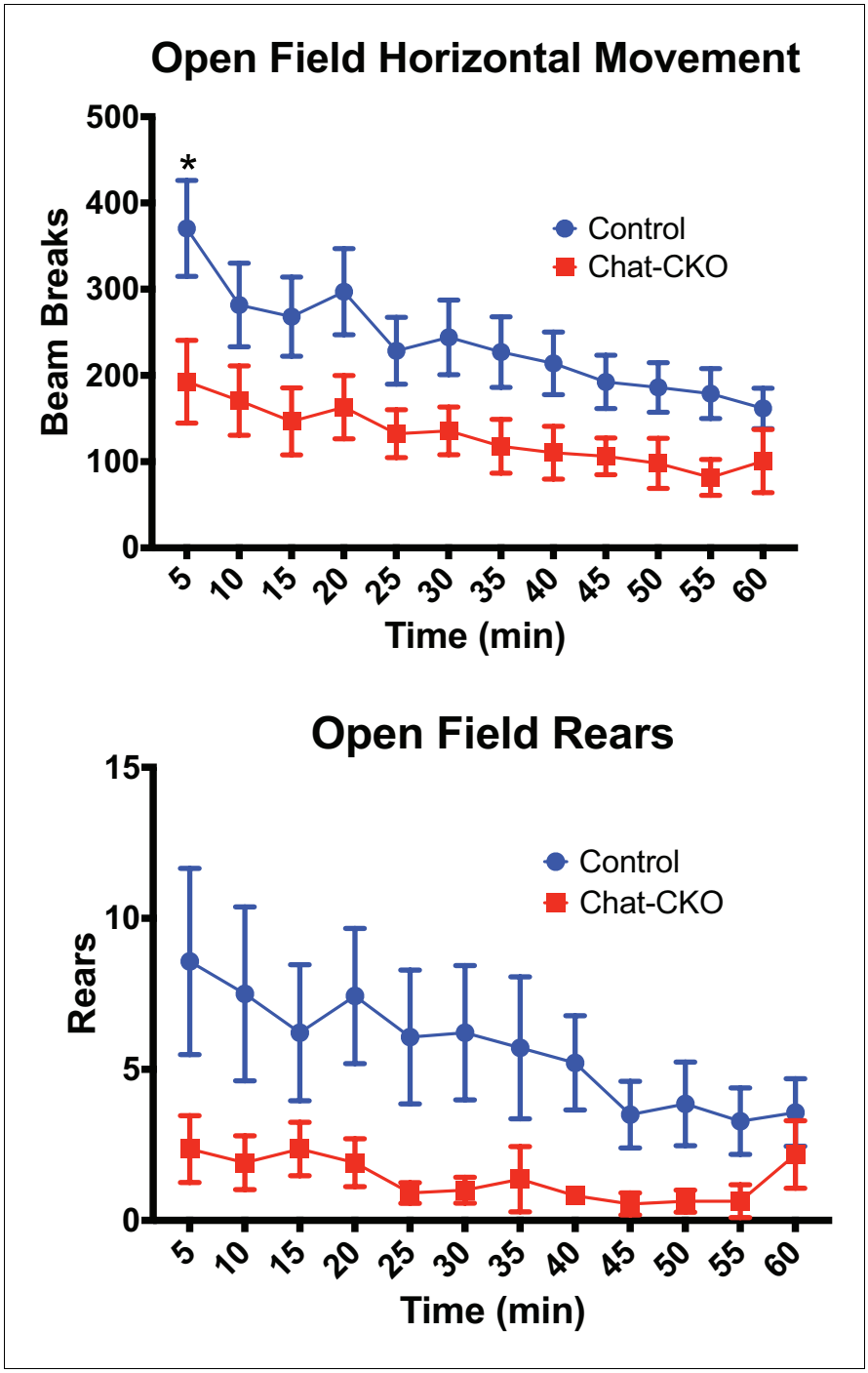

Figure 3—figure supplement 2. ChAT-CKO mice are significantly hypoactive. (Upper panel) Open field analysis of horizontal movements (two-way repeated measures ANOVA main effect of genotype $F_{(1,23)}$=5.498, p=0.02, time $F_{(11,253)}$=9.222, p<0.0001, interaction $F_{(11,253)}$=0.899, p=0.541, post-hoc Sidak's multiple comparisons test). (Lower panel) Open field analysis of vertical rearing movements (two-way repeated measures ANOVA main effect of genotype $F_{(1,23)}$=4.413, p=0.046, time $F_{(11,253)}$=2.452, p=0.0063, interaction $F_{(11,253)}$=0.987, p=0.458).
DOI: https://doi.org/10.7554/eLife.36691.012